

PROPERTIES OF ACTIVE CARBON WITH VARIOUS PARTICLE SHAPES OBTAINED IN CHAR-STEAM REACTION

Bronisław Buczek*

AGH University of Science and Technology, Faculty of Energy and Fuels,
al. Mickiewicza 30, 30-059 Cracow, Poland

The porous structure of cylindrical and ring-shaped char material was developed by partial steam gasification. Micropore and mesopore structures of active carbons with various forms of burn-off were evaluated by nitrogen adsorption/desorption isotherms. Parameters of the Dubinin-Radushkevich equation were calculated as well as the micropore size distribution by the Horvath-Kawazoe method. The results of textural investigations showed that more uniform micropore structure and better mechanical properties were found for ring-shaped active carbons.

Keywords: partial gasification, ring and cylindrical particles, active carbons, porous structure, surface area

1. INTRODUCTION

Carbon adsorbents in the form of granules, extrudates, powders (Bansal and Goyal, 2005), spheres (Banghel et al., 2011), bricks (Cacciola et al., 1995; Kierzak et al., 2007; Buczek, 2011) and with cylindrical shape (Wang et al., 2008) can be produced from suitable carbonaceous precursors by either physical or chemical routes (Tongpootorn et al., 2011).

The process of physical activation in order to obtain carbonaceous adsorbents, including active carbons, consists in a partial gasification of coal residue (char) by means of gases containing oxygen in their molecules. In industrial-scale processes, the oxidising agents that are most often employed are: water steam and carbon dioxide. They are, particularly steam, inexpensive and easily available. During gasification, mainly endothermic reactions of moderate rates proceed. Water steam and carbon dioxide react with char in the temperature range 750 °C to 950 °C. Endothermic reactions of gasification may be controlled in such a way that the process rate optimal for the formation of a microporous structure in the active carbon particles is not exceeded (Buczek, 1999). Steam reacts faster with char compared to carbon dioxide. The molecule of H₂O is characterised by high polarity, whereas CO₂ molecule is practically non-polar. The size of H₂O molecule (McClellan and Harnsberger, 1967) its viscosity coefficient (Bretsznajder, 1972), and its diffusion coefficient are greater than those of CO₂ (Makhorin, Glukhomanyuk, 1983). The properties of both gases are summarised in Table 1.

The product being formed upon activation, carbon monoxide does not impede steam gasification. Carbon monoxide may react with water vapour in pores according to the scheme: $\text{CO} + \text{H}_2\text{O} = \text{CO}_2 + \text{H}_2$. The diffusion coefficient of molecular hydrogen is by an order higher than those for carbon monoxide and dioxide. All this would favour easier and deeper water steam transport into the structure of char and the formation of microporous structure of active carbon.

*Corresponding author, e-mail: bbuczek@agh.edu.pl

Moreover, if we compare activation and dissociation energies, and relative reaction rate for both gases, we could evaluate their suitability for use in the gasification of carbonaceous materials (Table 2) (Makhorin and Glukhomyuk, 1983).

Table 1. Physico-chemical properties of water steam and carbon dioxide

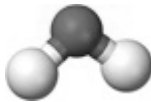
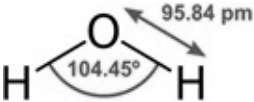

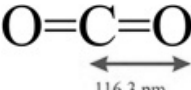
Compound	Molecule model	Molecule size [pm]	Cross-section area, ω_{cz} [nm ²]	Viscosity $\mu \times 10^3$ [Pa·s]	Diff. coeff. [cm ² ·s ⁻¹]
Water			12.8 ± 5.4 at -20 to 30°C	35.0 ± 0.01 t = 800°C	≈ 0.2
Carbon dioxide			20.3 ± 2.1 at -78 to 35°C	55.0 ± 0.02 t = 800°C	≈ 0.13

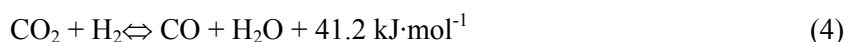
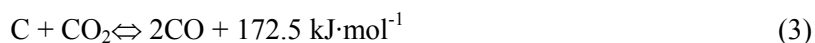
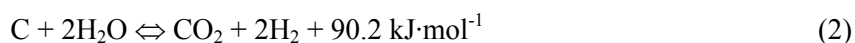
Table 2. Activation and dissociation energies and relative reaction rates with H₂O or CO₂

Reaction of carbon with gas	Activation energy [kJ·mol ⁻¹]	Dissociation reaction	Dissociation energy [kJ·mol ⁻¹]	Reaction rate 800 °C and 1 atm
C + H ₂ O = CO + H ₂	334.8	H ₂ O → H ₂ + O	485.5	3
C + CO ₂ = 2CO	359.9	CO ₂ → CO + O	527.4	1

To summarise, there are properties of the gas phase such as viscosity, diffusion coefficient and molecule size that would favour better transport of water steam inside the char and the reaction products in the opposite direction compared with carbon dioxide, which would affect the more advantageous kind of the structure inside the adsorbent particles. Nonetheless, the reaction rate with H₂O is three times higher than that with CO₂, which narrows the so-called kinetic regime of reaction. A compensating action of various effects is most probably the reason that no significant differences are observed in the porous structure of active carbons obtained by steam gasification compared with carbon dioxide one. Among the reactions occurring in the system carbon - steam in the process of adsorbent production, the basic one is the reaction of carbon monoxide and hydrogen formation presented by the equation:



Beside reaction (1), under atmospheric pressure and the process conditions, the following reactions also occur:



The last reaction is called water gas reaction or carbon monoxide reaction, and it is also the source of CO₂ in gaseous products. Reaction (4) occurs without volume change and hence the equilibrium does not depend on the pressure. Figure 1 presents temperature dependence of a theoretical equilibrium composition of the gas phase formed as a result of reactions (1-4).

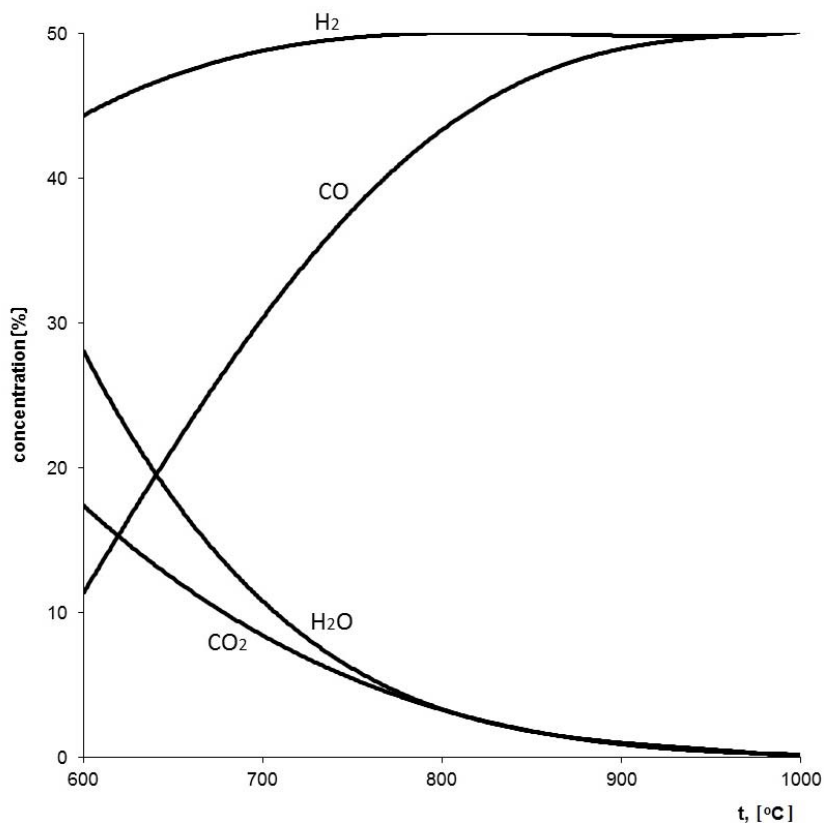


Fig. 1. Equilibrium gas composition for the reaction steam – carbon substance (Makhorin and Glukhmanyuk, 1983)

Upon the interaction of steam with carbon, the reactions (1) and (4) proceed inseparably and simultaneously. In the reaction products, at equilibrium conditions, both carbon oxides (CO and CO₂) appear simultaneously along with hydrogen. The reaction course depends on temperature. At temperatures exceeding 1000 °C, in gasification products, only hydrogen and carbon monoxide are present, which means that the reaction of water steam with carbon is described by reaction (1). Along with lowering the temperature, the concentration of CO and H₂ decreases, and H₂O and CO₂ contents increase. At temperatures below 810 °C, the reaction (2) proceeds towards the formation of carbon dioxide and hydrogen. At equilibrium at temperatures below 600 °C, the concentration of CO₂ exceeds that of CO. Thermodynamic analysis of steam gasification reactions allows to estimate the direction of the process, the effect of side and secondary reactions, the gas composition at equilibrium and heat effects. The kinetics of the process and real ratios between the components of the final products resulting from the distance from equilibrium for individual reactions still remain unknown.

The kinetics of steam gasification of a carbon substance consists of the following steps:

- transport of the water steam by diffusion from the gas phase onto the outer surface of particles,
- diffusion in particle pores,
- sorption of water vapour at the inner surface,
- proper chemical reaction,
- desorption of reaction products,
- diffusion of reaction products from the surface to the gas phase.

The above steps proceed either consecutively or simultaneously. If heat effects accompany these steps, reaction surface rise and porosity increase occurring with the proceeding process of adsorbent shaping are taken into account, then it is obvious that the mechanism of the process and its kinetics are extremely complex.

The aim of this work was to evaluate experimentally the effect of steam gasification on the properties of active carbons obtained from coal-char having different particle geometry (cylindrical and ring-shaped). Both types of particles were subjected to partial gasification at the same processing conditions.

2. EXPERIMENTAL

The studies were carried out on char formed by shaping a mixture of pulverised hard coal and wood tar at the spinning nozzle of 4.0 mm size, dried at the temperature of 180 °C and carbonised at the temperature of 600 °C, which originally was used for production commercial active carbon type N (Poland).

From the char, by means of mechanical treatment, cylinder-shaped particles were obtained (BDK) of 4.0 × 4.0 mm size and rings (DK) of inner diameter 0.8 mm and the outer size the same as for the cylinders.

The technical and chemical analyses of the char gave the following results: moisture content: $W^a = 4.1\%$; ash: $A^a = 8.2\%$; volatiles: $V^a = 14.7\%$; carbon: $C^a = 74.5\%$; hydrogen: $H^a = 2.17\%$; sulphur: $S^a = 0.62\%$; nitrogen: $N^a = 2.06\%$.

The process was carried out in a reactor with a particle monolayer (Jankowska et al., 1991), the schematic diagram of which is presented in Fig. 2.

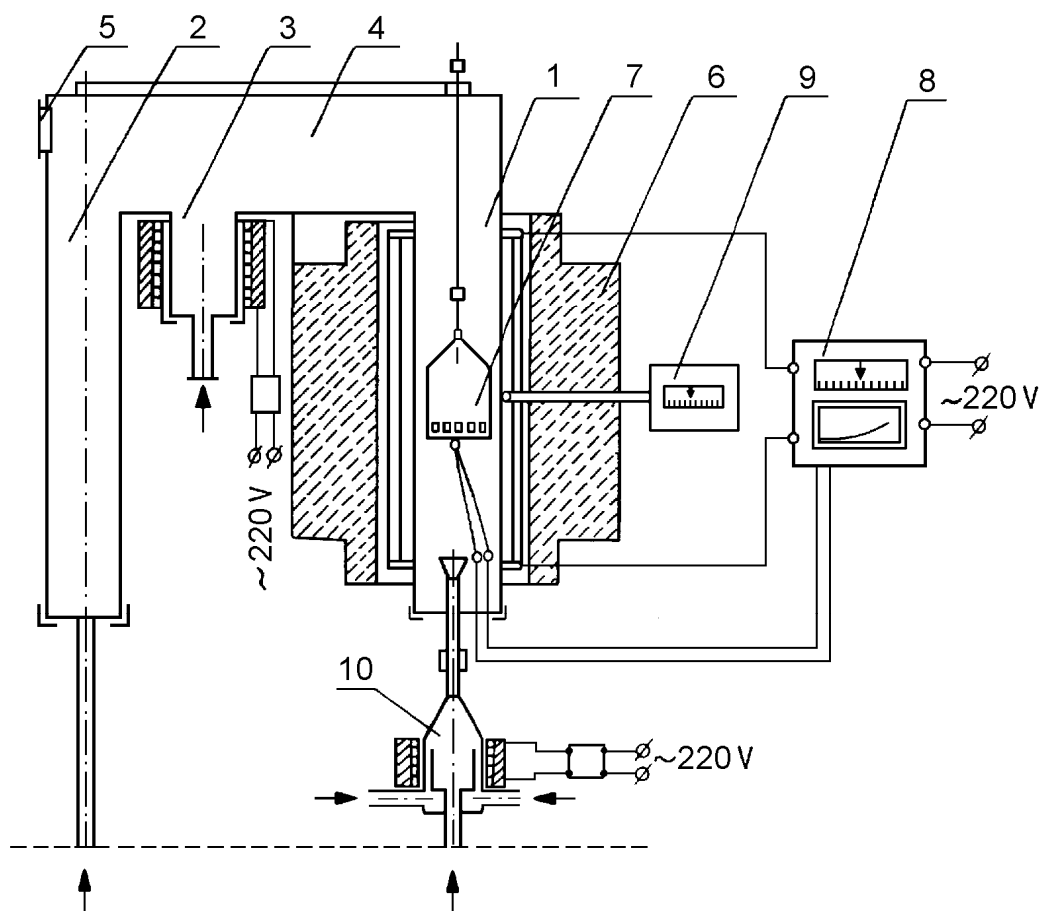


Fig. 2. Monolayer reactor used for steam activation process;

- 1 - reactor, 2 - cooling space, 3 - sample preheating, 4 - connecting channel, 5 - entry samples, 6 - furnace, 7 - basket, 8 - temperature control and recording, 9 - temperature meter, 10 - gas mixer

The flow of superheated steam was $0.01556 \text{ g}\cdot\text{cm}^{-2}\cdot\text{s}^{-1}$, and the process temperature $850 \text{ }^\circ\text{C}$. From the gasification reaction two series of active carbons were obtained, cylindrical (BD1-BD4) and rings (D1-D4), for which the conversion degree (burn-off) ranged between 45.31 and 72.04.

3. RESULTS AND DISCUSSIONS

3.1. Density and porosity

Significant properties of adsorbents include their densities, mainly, apparent and real densities (Webb and Orr, 1997) In the present work, the apparent density of both series of active carbons was determined by the mercury method, and the real density was determined by the helium method using an AccuPyc 1330 pycnometer. Knowing helium and mercury densities, the pore volume for both series of active carbons could be calculated. The results of analyses and calculations along with the kinetic data are summarised in Table 3.

Table 3. Reaction time, conversion (burn-off) degree and properties of active carbons

Active carbon	Reaction time [min]	Conversion degree [%]	Mercury density [$\text{g}\cdot\text{cm}^{-3}$]	Helium density [$\text{g}\cdot\text{cm}^{-3}$]	Pore volume [$\text{g}\cdot\text{cm}^{-3}$]
BDK	0	0	1.077	1.790	0.370
BD1	30	45.31	0.890	1.802	0.675
BD2	38	53.26	0.845	1.898	0.656
BD3	45	61.70	0.737	1.993	0.856
BD4	57	72.04	2.210	0.766	
DK	0	0	1.119	1.790	0.328
D1	27	47.98	0.819	1.938	0.705
D2	31	52.44	0.789	2.094	0.790
D3	39	60.00	0.692	2.125	0.975
D4	47	71.98	0.626	2.206	1.145

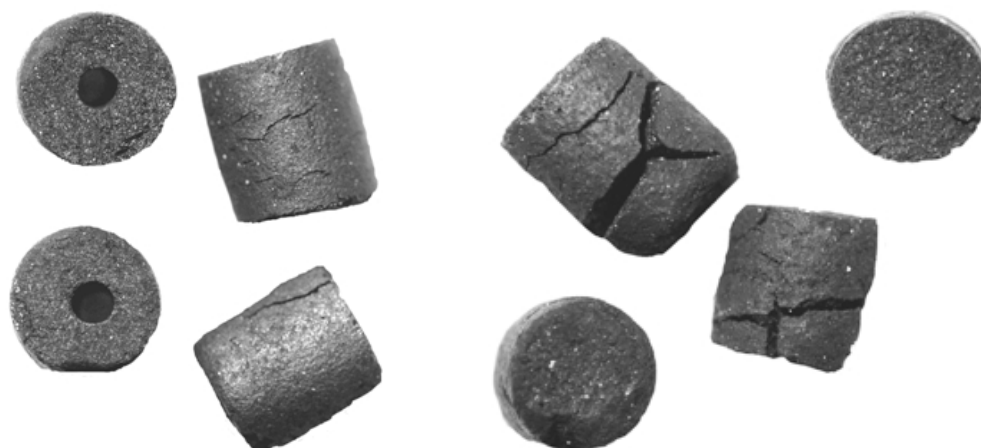


Fig. 3. The state of outer surface of cylindrical and ring-shaped particles

In the case of active carbons of series D, an increase in helium density and a decrease in mercury density, and a rising pore volume are observed with time. It proves the advantageous outcome of gasification of the ring shapes. The cylindrical carbons of series BD crack in a short time, which is evidently reflected in the values of both densities, and consequently irregularly varying total pore volume. Fig. 3 presents the outer surface of particles of a different shape and of a similar conversion degree ($D_2 = 52.44$, $BD_2 = 53.26$).

3.2. Pore structure analysis

The pore structure of active carbons was analysed based on low temperature nitrogen adsorption studies. The isotherm was determined by the volume method using a Sorptomatic 1900 instrument. Automatic control of dosing and of the amount adsorbed of the adsorbate employed allowed of programme the amount and the distribution of experimental points. The measurements were performed at the temperature of -195.5°C at the range of relative pressures $p/p_0 = 0.00001 - 0.999$. Figures 4 and 5 present the adsorption-desorption isotherms.

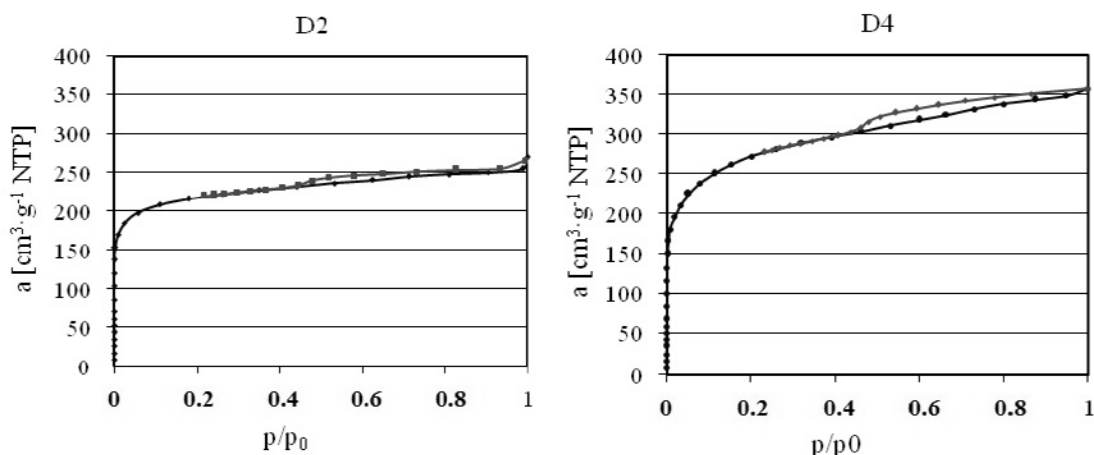


Fig. 4. Nitrogen adsorption isotherms for active carbons D2 and D4

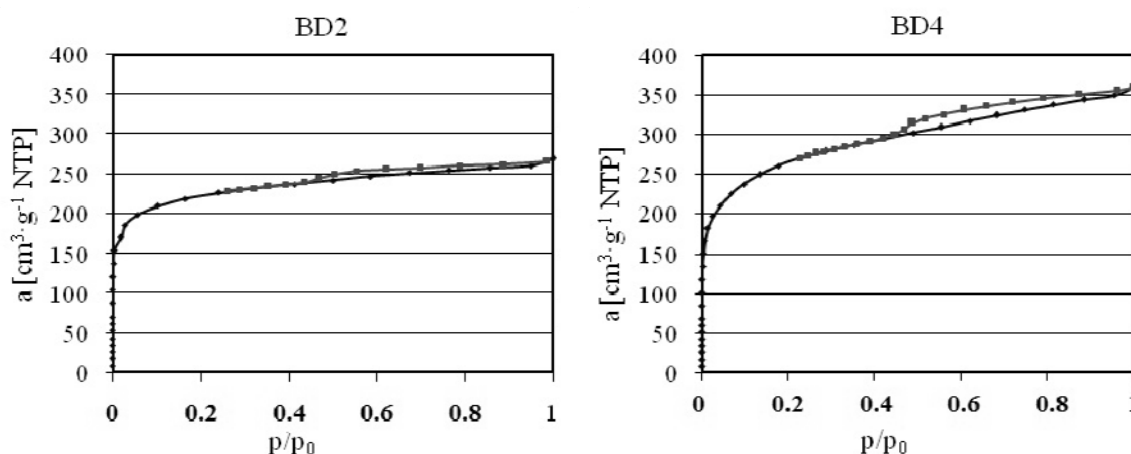


Fig. 5. Nitrogen adsorption isotherms for active carbons BD2 and BD4

All the isotherms show the Langmuir behaviour of rising adsorption in the low pressure range and a hysteresis loop, which proves that mainly microporous and a small degree mesoporous structures

develop in the activation conditions. From the obtained data, parameters characterising the microporous structure, W_0 , and the characteristic energy, E_0 , from the Dubinin-Radushkevich equation (Dubinin, 1987) were determined. From the micropore volume and the amount of adsorbed nitrogen, the formal surface area of micropores, S_{DR} , was calculated. To determine the distribution of micropore volume based on nitrogen isotherm, a method proposed by (Horvath and Kawazoe, 1983) was applied, and from their distribution, the half-width of slot-like pores, x_{HK} , was determined. The surface area of mesopores, S_{me} , was calculated with a method proposed by (Dollimore and Heal, 1964) and the specific surface area, S_{BET} , from the Brunauer, Emmet and Teller equation (Bansal and Goyal, 2005). The calculation and analyses results are summarised in Table 4.

Table 4. Analysis of micropore structure and surface area of active carbons

Active carbon	W_0 [cm ³ ·g ⁻¹]	E_0 [kJ·mol ⁻¹]	S_{DR} [m ² ·g ⁻¹]	x_{HK} [nm]	S_{me} [m ² ·g ⁻¹]	S_{BET} [m ² ·g ⁻¹]
BD1	0.256	23.6	715	0.463	45	595
BD2	0.313	20.8	881	0.475	77	765
BD3	0.346	19.0	976	0.485	111	837
BD4	0.368	17.2	1035	0.495	158	927
D1	0.282	21.6	795	0.486	49	636
D2	0.313	20.9	883	0.487	72	779
D3	0.320	18.9	902	0.493	96	812
D4	0.374	17.6	1054	0.485	150	962

The active carbons of the highest conversion degree demonstrate the most developed pore structure. The specific surface area and the mesopore surface area of the active carbons BD4 and D4 are comparable. Along with the burn-off, a fall in the value of characteristic energy E_0 occurs for carbons of both the series D and BD. It is associated with an increase in the micropore size, x_{HK} , chiefly for series BD. This is confirmed by changes in the micropore volume distribution and in their size functions. For series BD, a decrease in the maximum value and broadening of the curve occurs – the volume of larger pores increases (Fig. 6). In the case of series D carbons, only the micropore volume decreases, whereas their size, x_{HK} , remains approximately constant. It proves that the activation of ring-shaped particles may yield a more uniform micropore structure.

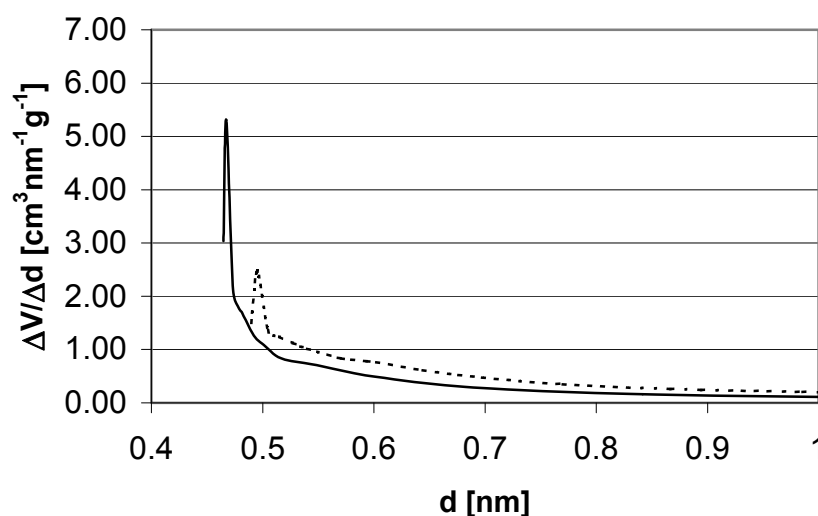


Fig. 6. Micropore distribution as a function of size for BD1 (solid) and BD4 (dashed line)

3.3. Evaluation of pressure drop in the bed of cylindrical and ring-shaped active carbons

Pressure drop across the bed packed with cylinders (4 × 4 mm) and rings of the same size and inner diameter of 0.8 mm, at the same gas flow conditions was assumed. The calculations were conducted with the assumption that the elements are packed in a column of 1 m in height and 1 m in diameter. The pressure drops, Δp , were calculated using a modified Darcy-Weisbach (Koch and Noworyta, 1992) and Zhavoronkov (Paderewski, 1998) equations. Parameters characterising the packing were calculated, such as porosity, outer surface area and hydraulic diameters of the elements. Their values are presented in Table 5.

Table 5. Parameters characterising active carbons

Parameter	Cylinders	Rings
Hydraulic diameter of element, d_{zs} [m]	$4.003 \cdot 10^{-3}$	$3.43 \cdot 10^{-3}$
Porosity, ε [-]	0.084	0.12
Outer surface area, a_s [m ² /m ³]	1500	1750

After calculating and comparing Reynolds numbers for individual cases, it appeared that the Reynolds number for cylinders is higher than the Reynolds number for rings by about 12% when calculated from Darcy-Weisbach equation and by nearly 16% when using Zhavoronkov equation. The obtained Reynolds numbers were used to calculate and compare the values of friction factors λ_f and λ_z .

$$\lambda_f = \frac{150}{Re} + 1.75 \quad (5)$$

$$\lambda_z = \frac{140}{Re} \quad \text{for } Re \leq 40 \quad (6)$$

$$\lambda_z = \frac{16}{Re^{0.2}} \quad \text{for } Re > 40 \quad (7)$$

On the assumption that the values of Reynolds numbers range from 1 to 3000, the values of the friction factors λ_f for the rings are from 0.3 to 10% higher than the values of the friction factors for the cylinders. In the case of calculating the friction factors λ_z according to Zhavoronkov equation, the differences in the values range from 13% for laminar flow and ca. 3% for turbulent flow. A comparison of flow resistance values across the bed ($\Delta p_c / \Delta p_p$) is presented in Figs. 7 and 8.

When calculating pressure drops using the Darcy-Weisbach formula it appears that the difference between flow resistance values increases with the increase in the Reynolds number. The flow resistance across the bed of cylindrical-shaped elements is from about 2.3 to about 2.6 times higher than that across the bed of ring-shaped elements. The calculation results of pressure drops according to Zhavoronkov equation also indicate that for a bed of cylindrical-shaped elements, the flow resistance is from 2.15 times higher for $Re \leq 40$ and about 2.42 times for $Re > 40$.

Moreover, the calculation results demonstrate that the ratio between the pressure drop across the cylindrical-shaped elements and the pressure drop across the bed of ring-shaped elements is higher than 1 in each case. This means that at the same size and column operating conditions, the flow resistance for the ring packed bed will always be lower than that across the cylindrical packed bed.

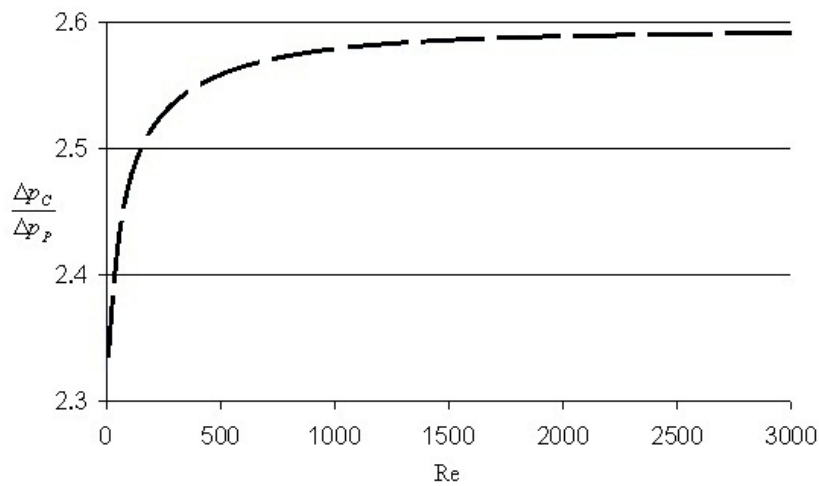


Fig. 7. Flow resistance values *versus* Re according to Darcy-Weisbach equation

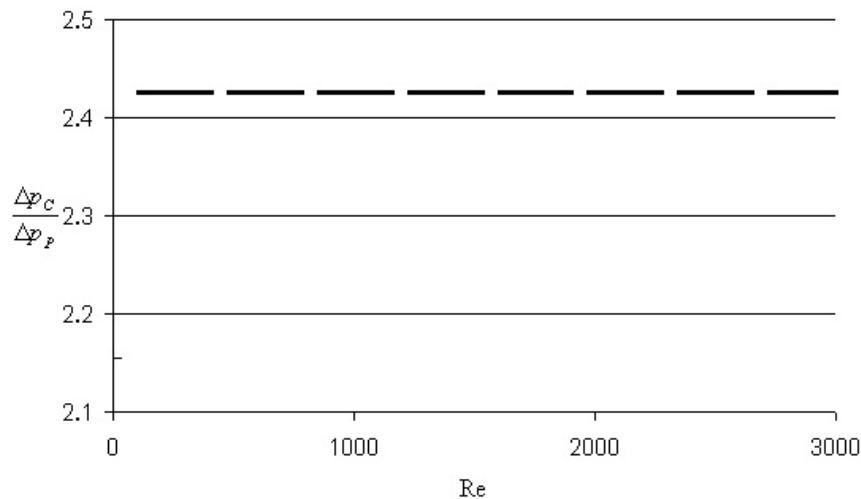


Fig. 8. Flow resistance values *versus* Re according to Zhavoronkov equation

4. CONCLUSIONS

The studies carried out demonstrate how the geometry of the particle affects the properties of active carbons formed in the reaction of steam with coal char. The steam activation leads to a faster development of the texture of ring-shaped particles, hence also the process kinetics along with a small increase in the specific surface area and the surface area of mesopores. The size of micropores in ring-shaped particles of different conversion degree (burn-off) remains practically stable. It means that molecular-sieve properties occur in active carbons prepared in this way and shows that the reaction proceeds precedes close to the kinetic zone. A bigger fraction of the micropore volume is also observed, and, what follows, a higher adsorption capacity for small molecule adsorbates. Ring-shaped active carbons are characterised by better strength parameters compared with cylindrical particles. Owing to the different shape, flow resistance through the bed of ring-shaped particles is lower than that for the bed of cylindrical particles.

The author is grateful to the AGH (Project 11.11.210.218) for partial financial support of this work

REFERENCES

- Banghel A., Singh B., Prasad G.K., Pandlej P., Gutch P.K., 2011. Preparation and characterization of active carbon spheres prepared by chemical activation. *Carbon*, 49, 4739-4744. DOI: 10.1016/j.carbon.2011.06.080.
- Bansal R.C., Goyal M., 2005. *Activated carbon adsorption*, CRC Press Taylor&Francis Group, Boca Raton, FL USA, 85-101.
- Bretznajder St., 1972. *Properties of liquids and gases*. WNT Warszawa, 502-513 (in Polish).
- Buczek B., 1999. The influence of properties within particles of active carbons on selected adsorption processes. *Studies Surf. Sci. Catal.*, 120A, 507-530. DOI: 10.1016/S0167-2991(99)80563-1.
- Buczek B., 2011. Nanostructural materials for energy storage systems. *Int. J. Photoenergy*, 2011, Article ID 340540. DOI: 10.1155/2011/340540.
- Cacciola C., Restuccia, Mercadante L., 1995. Composites of activated carbon for refrigeration adsorption machines. *Carbon*, 33, 1205-1210. DOI: 10.1016/0008-6223(95)00051-E.
- Dollimore D., Heal G.R., 1964 An improved method for the calculation of pore size distribution from adsorption data. *J. Appl. Chem.*, 14, 109-116. DOI: 10.1002/jctb.5010140302.
- Dubinin M.M., 1987, Adsorption properties and microporous structures of carbonaceous adsorbent. *Carbon*, 25, 593-598. DOI: 10.1016/0008-6223(87)90208-9.
- Horvath G., Kawazoe K. J., 1983. Method for the calculation of effective pore size distribution in molecular sieve carbon. *J. Chem. Eng. Japan*, 16, 470-475. DOI: 10.1252/jcej.16.470.
- Jankowska H., Świątkowski A., Choma J., 1991. *Active carbon*. Ellis Horwood, New York, 25-30.
- Kierzak K., Machnikowska H., Gryglewicz G., Machnikowski J., 2007. Methane storage capacity of monoliths made of activated carbons of different porosity development. *International Conference on Coal Science and Technology*. Nottingham, UK, 28-31.08.2007, CD-ROM.
- Koch R., Noworyta A., 1992. *Mechanical processes in chemical engineering*. WNT, Warszawa, 189-192 (in Polish).
- Makhorin K.E., Glukhomanyuk A.M., 1983. *Preparation of carbon adsorbents in a fluidised bed*. Naukova Dumka, Kiev, 9-12 (in Ukrainian).
- McClellan A. L., Harnsberger H. F., 1967. Cross-sectional areas of molecules adsorbed on solid surfaces. *J. Colloid Interface Sci.*, 23, 577-599. DOI: 10.1016/0021-9797(67)90204-4.
- Paderewski M. L., 1999. *Adsorption processes in chemical engineering*. WNT, Warszawa, 27-31 (in Polish).
- Tongpoothorn W., Sriutta M., Homchan P., Chanthai S., Ruangviriyachai C., 2011. Preparation of activated carbon derived from *Jatropha curcas* fruit shell by simple thermo-chemical activation and characterization of their physico-chemical properties. *Chem. Eng. Res. Des.*, 89, 335-340. DOI: 10.1016/j.cherd.2010.06.012.
- Wang J.-C., Liu Q.-Y., Liu Z.-Y., Huang Z.-G., 2008. Heterogeneity of V₂O₅ supported cylindrical activated coke used for SO₂ removal from flue gas. *Chem. Eng. Technol.*, 31, 1056-1060. DOI: 10.1002/ceat.200700332.
- Webb P., Orr C., Camp R.W., Olivier J.P., 1997. *Analytical methods in fine particle technology*. Micromeritics Instrument Corporation, Norcross, GA USA, 193-218.

Received 26 January 2012

Received in revised form 13 July 2012

Accepted 15 July 2012